

# Nonadiabatic charged spherical evolution in the postquasistatic approximation

L. Rosales,<sup>1</sup> W. Barreto,<sup>2</sup> C. Peralta,<sup>3,4</sup> and B. Rodríguez-Mueller<sup>5</sup>

<sup>1</sup>*Laboratorio de Física Computacional, Universidad Experimental  
Politécnica “Antonio José de Sucre”, Puerto Ordaz, Venezuela*

<sup>2</sup>*Centro de Física Fundamental, Facultad de Ciencias, Universidad de Los Andes, Mérida, Venezuela\**

<sup>3</sup>*Deutscher Wetterdienst, Frankfurter Str. 135, 63067 Offenbach, Germany*

<sup>4</sup>*School of Physics, University of Melbourne, Parkville, VIC 3010, Australia*

<sup>5</sup>*Computational Science Research Center, College of Sciences,  
San Diego State University, San Diego, California, USA*

We apply the postquasistatic approximation, an iterative method for the evolution of self-gravitating spheres of matter, to study the evolution of dissipative and electrically charged distributions in General Relativity. The numerical implementation of our approach leads to a solver which is globally second-order convergent. We evolve nonadiabatic distributions assuming an equation of state that accounts for the anisotropy induced by the electric charge. Dissipation is described by streaming out or diffusion approximations. We match the interior solution, in noncomoving coordinates, with the Vaidya–Reissner–Nordström exterior solution. Two models are considered: i) a Schwarzschild-like shell in the diffusion limit; ii) a Schwarzschild-like interior in the free streaming limit. These toy models tell us something about the nature of the dissipative and electrically charged collapse. Diffusion stabilizes the gravitational collapse producing a spherical shell whose contraction is halted in a short characteristic hydrodynamic time. The streaming out radiation provides a more efficient mechanism for emission of energy, redistributing the electric charge on the whole sphere, while the distribution collapses indefinitely with a longer hydrodynamic time scale.

PACS numbers: 04.40.Nr, 04.25.-b, 04.25D-

## I. INTRODUCTION

Despite their apparent simplicity, 1+1 models of the fluid dynamics of compact objects in numerical relativity can include realistic transport mechanisms and equations of state. Renewed interest on electric charge in stars has driven the numerical integration of the Einstein–Maxwell (EM) system. Current integrators of the EM system are in comoving coordinates [1], and seem to be limited to one dimensional numerical solvers [2], [3] of the May and White family [4], [5]. Because of the obvious interest in three-dimensional situations, it is desirable to use noncomoving coordinates. Numerical simulations to explore the relevance of electric charge in the process of dissipative and anisotropic (viscous) gravitational collapse are desirable as well.

The numerical solution of Einstein equations in 3+1 dimensions is an essential tool for the investigation of strong field scenarios of astrophysical interest (see [6] and references therein). Numerical relativity has led to the discovery of critical phenomena in gravitational collapse [7], allowed the study of binary black holes and neutron stars [8]–[11] and the development of relativistic hydrodynamics solvers [12], among other major achievements. The main limitation currently faced by realistic models in numerical relativity is the computational demand in three-dimensional evolution. Computationally less in-

tensive 1D models still remain an interesting alternative and help narrow the search in the parameter space for general solvers. These simplified systems provide a necessary test bed to study the phenomena expected in fully realistic three-dimensional configurations.

In this paper, we study a self-gravitating spherical distribution of charged matter containing a dissipative fluid. We use noncomoving coordinates and follow the method reported in [14]. Herrera et al. realized that this method was equivalent to going one step further from the quasistatic regime, and consequently has been named the postquasistatic approximation (PQSA) after [15].

The essence of the PQSA was first proposed in [16] using radiative Bondi coordinates and it has been extensively used by Herrera and collaborators [17]–[22]. In the context of charged distributions of matter the original method was used as well [23], [24], [25]. The approach is based on the introduction of a set of conveniently defined “effective” variables, which are the effective pressure and energy density, and a heuristic ansatz on the latter [14]. By QSA we mean that the effective variables coincide with the corresponding physical variables (pressure and energy density). In Bondi coordinates the notion of QSA is not evident: the system goes directly from static to postquasistatic evolution. In an adiabatic and slow evolution we can catch-up that phase, clearly seen in noncomoving coordinates; this can be achieved using Schwarzschild coordinates [15]. If the configuration is leaving equilibrium, the PQSA description seems to be enough and can be used as a test bed in numerical relativity [26]. Its systematic use of local Minkowskian and comoving observers, named Bondians, was used to

---

\*On sabbatical leave at Universitat de les Illes Balears, Palma de Mallorca, Spain.

reveal a central equation of state in adiabatic scenarios [27], and to couple matter with radiation [28].

In self-gravitating systems the electric charge is believed to be constrained by the fact that the resulting electric field should not exceed the critical field for pair creation,  $10^{16} \text{ V cm}^{-1}$  [29]. This restriction in the critical field has been questioned [30]–[33] and does not apply to phases of intense dynamical activity with time scales of the order of (or even smaller than) the hydrostatic time scale, and for which the QSA [34] is clearly not reliable as in the collapse of very massive stars or the quick collapse phase preceding neutron star formation (see [35] and references therein). Electric charge has been also studied mostly under static conditions [35], [36], [37], [38]. It is of recent interest the charged quasiblack holes [39] and its extension to quasispherical realization [40]. Distributions electrically charged can be considered in practice as anisotropic [41], [42]. Authors combine anisotropy and electric charge [35], [43], [44] but not as a single entity by means of an equation of state.

The electric field has been postulated to be very high in strange stars with quark matter [45], [46], although other authors suggest that strange stars wouldn't need a large electrical field [47]. The effects of dissipation, in both limiting cases of radiative transport, within the context of the QSA, have been studied in [48]. Using this approximation is very sensible because the hydrostatic time scale is very small, compared with stellar lifetimes, for many phases of the life of a star. It is of the order of 27 minutes for the sun, 4.5 seconds for a white dwarf and 104 seconds for a neutron star of one solar mass and 10 Km radius [49]–[50]. However, such an approximation does not apply to the very dynamic phases mentioned before. In those cases it is mandatory to take into account terms which describe departure from equilibrium, i.e. a full dynamic description has to be used [51].

In this paper we consider that the electric charge can be seen as anisotropy [41], but not any anisotropy as we shall see. For certain density ranges, locally anisotropic pressure can be physically justified in self-gravitating systems, since different kinds of physical phenomena may take place, giving rise to local anisotropy and in turn relaxing the upper limits imposed on the maximum value of the surface gravitational potential [52]. The influence of local anisotropy in general relativity has been studied mostly under static conditions (see [53] and references therein; [54]). Herrera et al. [55] have reported a general study for spherically symmetric dissipative anisotropic fluids with emphasis on the relationship among the Weyl tensor, the shear tensor, the anisotropy of the pressure and the density inhomogeneity.

On the other hand, it is well known that different energy-momentum tensors can lead to the same space-time [56]–[60]. For instance, viscosity can be considered as a special case of anisotropy [61]. Here we illustrate this idea for the Einstein-Maxwell system under spherical symmetry. To accomplish that program we use the total energy characterization as in [29] and [62]. The elec-

tric energy (or pressure) contributes to the fluid in a such way that the electrically charged perfect fluid is equivalent to an anisotropic fluid under certain conditions.

Massive stars evolve emitting massless particles (photons and/or neutrinos). Neutrino emission seems to be the only plausible mechanism to carry away the bulk of binding energy of a collapsing star, leading to a black hole or neutron star [63]. It seems clear that the free-streaming process is associated with the initial stages of the collapse, while the diffusion approximation becomes valid toward the final stages. Observation from supernova 1987A indicates that the regime of radiation transport prevailing during the emission process is closer to the diffusion approximation than to the free streaming [64]. Heat flow is usually considered as proportional to the gradient of temperature. This assumption is very sensible because the mean free path of particles responsible for the propagation of energy in stellar interiors is very small as compared with the typical length of the object [34].

Although some transport equations in the relaxation time approximation have been proposed (see for instance [65] and references therein), the evolution of temperature profiles in the context of general relativity remains an unsolved problem. Therefore, we avoid stating any explicit evolution equation for heat flow in this investigation. Recently, some progress have been achieved by Herrera and collaborators on the study of dissipation via an appropriate causal procedure (see for example [55, 66–68]). In the present investigation we obtain the zeroth order level of approximation for heat flow profiles, which will serve as the basis of a future investigation which includes dissipation in a realistic way using the Müller-Israel-Stewart theory [69–72]. We already see an important advantage using the PQSA studying configurations with anisotropy (induced by shear viscosity), streaming out and heat flow processes in spherical collapse: an observer using radiating coordinates to study heat flow misses some important details.

The paper is organized as follows. In Sec. II we write the field equations for Bondian observers to show how the electric charge induces anisotropy, matching with the exterior Reissner-Nordström-Vaidya solution, and write the surface equation, following the PQSA protocol [15], [73]. In Sec. III we present a summary of the numerical methods employed. In Sec. IV we show local and global tests of numerical convergence and illustrate the PQSA integration procedure with two nonadiabatic charged models. In Sec. V we conclude with some remarks.

## II. THE EINSTEIN-MAXWELL SYSTEM

### A. Field equations for Bondian observers

To write the Einstein field equations we use the line element in Schwarzschild-like coordinates

$$ds^2 = e^\nu dt^2 - e^\lambda dr^2 - r^2 (d\theta^2 + \sin^2 \theta d\phi^2), \quad (1)$$

where  $\nu = \nu(t, r)$  and  $\lambda = \lambda(t, r)$ , with  $(t, r, \theta, \phi) \equiv (0, 1, 2, 3)$ . In order to get physical input we introduce the Minkowski coordinates  $(\tau, x, y, z)$  by [74]

$$d\tau = e^{\nu/2} dt, \quad dx = e^{\lambda/2} dr, \quad dy = r d\theta, \quad dz = r \sin \theta d\phi. \quad (2)$$

In these expressions  $\nu$  and  $\lambda$  are constants, because they have only local values. Next we assume that, for an observer moving relative to these coordinates with velocity  $\omega$  in the radial direction, the space contains a nonstatic distribution of matter which is spherically symmetric and consists of charged fluid of energy density  $\rho$ , pressure  $p$ , electric energy density  $\rho_e$ , radiation energy flux  $q$  diffusing in the radial direction, and unpolarized radiation of energy density  $\epsilon$ . Thus, the energy-momentum tensor is

$$T_{\mu\nu} = (\rho + p)u_\mu u_\nu - pg_{\mu\nu} + \epsilon l_\mu l_\nu + q_\mu u_\nu + q_\nu u_\mu + E_{\mu\nu}, \quad (3)$$

where  $u_\alpha$ ,  $l_\alpha$ ,  $q_\alpha$  are the 4-velocity, the 4-null vector and the heat flux 4-vector respectively, which satisfy  $u^\alpha u_\alpha = 1$ ,  $q_\alpha u^\alpha = 0$ ,  $l^\alpha l_\alpha = 0$ , and  $E_{\mu\nu}$  is the electromagnetic energy-momentum tensor

$$E_{\mu\nu} = \frac{\pi}{4} \left[ F_\mu{}^\kappa F_{\nu\kappa} + \frac{1}{4} g_{\mu\nu} F_{\sigma\kappa} F^{\sigma\kappa} \right], \quad (4)$$

where  $F_{\mu\kappa}$  is the Maxwell field tensor, which satisfies the Maxwell equations:

$$F_{[\mu\nu;\sigma]} = 0 \quad (5)$$

and

$$(\sqrt{-g}F^{\mu\nu})_{;\nu} = 4\pi\sqrt{-g}J^\mu, \quad (6)$$

where the semicolon (;) and the comma (,) represent covariant derivative and partial differentiation with respect to the indicated coordinate, respectively;  $J^\mu = \sigma u^\mu$  is electric current 4-vector and  $\sigma$  the electric conductivity. Because of the spherical symmetry, only the radial electric field  $F^{tr} = -F^{rt}$  is nonzero. On the other hand, the inhomogeneous Maxwell equations become

$$s_{,r} = 4\pi r^2 J^t e^{\frac{1}{2}(\nu+\lambda)} \quad (7)$$

and

$$s_{,t} = -4\pi r^2 J^r e^{\frac{1}{2}(\nu+\lambda)}, \quad (8)$$

where  $J^t$  and  $J^r$  are the temporal and radial components of the current 4-vector, respectively. The function  $s(t, r)$

is naturally interpreted as the charge within the radius  $r$  at the time  $t$ . We define the function  $s(t, r)$  by  $F^{tr} = s e^{-(\lambda+\nu)/2}/r^2$ , with

$$s(t, r) = \int 4\pi r^2 J^t e^{-(\lambda+\nu)/2} dr. \quad (9)$$

The conservation of charge inside a sphere comoving with the fluid is expressed as

$$u^\alpha s_{,\alpha} = 0. \quad (10)$$

We can write the conservation equation in a more suitable form for numerical purposes

$$s_{,t} + \frac{dr}{dt} s_{,r} = 0, \quad (11)$$

where the velocity of matter in the Schwarzschild coordinates is

$$\frac{dr}{dt} = \omega e^{(\nu-\lambda)/2}. \quad (12)$$

The contravariant components of the 4-velocity, the heat flux 4-vector and the null outgoing vector are

$$u^\mu = \frac{e^{-\nu/2}}{(1-\omega^2)^{1/2}} \delta_t^\mu + \frac{\omega e^{-\lambda/2}}{(1-\omega^2)^{1/2}} \delta_r^\mu, \quad (13)$$

$$q^\mu = \frac{\omega e^{-\nu/2} q}{(1-\omega^2)^{1/2}} \delta_t^\mu + \frac{e^{-\lambda/2} q}{(1-\omega^2)^{1/2}} \delta_r^\mu \quad (14)$$

and

$$l^\mu = e^{-\nu/2} \delta_t^\mu + e^{-\lambda/2} \delta_r^\mu. \quad (15)$$

We write the field equations for the Einstein-Maxwell system in relativistic units ( $G = c = 1$ ) as follows:

$$\begin{aligned} \frac{\rho + p\omega^2}{1-\omega^2} + \frac{2\omega q}{1-\omega^2} + \frac{1+\omega}{1-\omega} \epsilon + \frac{s^2}{8\pi r^4} = \\ \frac{1}{8\pi r} \left[ \frac{1}{r} - e^{-\lambda} \left( \frac{1}{r} - \lambda_{,r} \right) \right], \end{aligned} \quad (16)$$

$$\begin{aligned} \frac{p + \rho\omega^2}{1-\omega^2} + \frac{2\omega q}{1-\omega^2} + \frac{1+\omega}{1-\omega} \epsilon - \frac{s^2}{8\pi r^4} = \\ \frac{1}{8\pi r} \left[ e^{-\lambda} \left( \frac{1}{r} + \nu_{,r} \right) - \frac{1}{r} \right], \end{aligned} \quad (17)$$

$$\begin{aligned} p + \frac{s^2}{8\pi r^4} = \\ \frac{1}{32\pi} \{ e^{-\lambda} [2\nu_{,rr} + \nu_{,r}^2 - \lambda_{,r}\nu_{,r} + \frac{2}{r}(\nu_{,r} - \lambda_{,r})] \\ - e^{-\nu} [2\lambda_{,tt} + \lambda_{,t}(\lambda_{,t} - \nu_{,t})] \} \end{aligned} \quad (18)$$

and

$$\begin{aligned} \frac{\omega}{1-\omega^2} (p + \rho) + \frac{(1+\omega^2)}{1-\omega^2} q + \frac{1+\omega}{1-\omega} \epsilon = \\ - \frac{\lambda_{,t}}{8\pi r} e^{-\frac{1}{2}(\nu+\lambda)}. \end{aligned} \quad (19)$$

### B. Anisotropy induced by electric charge

where

To write the field equations in a form equivalent to an anisotropic fluid, we introduce

$$e^{-\lambda} = 1 - 2\mu/r, \quad (20)$$

$$\mu(t, r) = m(t, r) - \frac{s^2}{2r}, \quad (21)$$

---

$m$  being the total mass [29], [62]. Thus the field equations (16)–(19) read

$$\tilde{\rho} = \frac{\mu_{,r}}{4\pi r^2}, \quad (22)$$

$$\tilde{p} = \frac{1}{8\pi r} \left[ \nu_{,r} \left( 1 - \frac{2\mu}{r} \right) - \frac{2\mu}{r^2} \right], \quad (23)$$

$$p_t = \frac{(r-2\mu)}{16\pi r} \left\{ \nu_{,rr} + \frac{\nu_{,r}^2}{2} + \frac{\nu_{,r}}{r} - \left( \nu_{,r} + \frac{2}{r} \right) \frac{(\mu_{,r} - \mu/r)}{(r-2\mu)} \right\} - \frac{e^{-\nu}}{8\pi(r-2\mu)} \left\{ \mu_{,tt} + \frac{3\mu_{,t}^2}{(r-2\mu)} - \frac{\mu_{,t}\nu_{,t}}{2} \right\} \quad (24)$$


---

and

$$S = -\frac{\mu_{,t}}{4\pi r} (1 - 2\mu/r)^{\frac{1}{2}} e^{-\frac{1}{2}\nu}, \quad (25)$$

where the conservative variables are

$$\tilde{\rho} = \frac{\hat{\rho} + p_r \omega^2}{1 - \omega^2} + \frac{2\omega q}{1 - \omega^2} + \epsilon \frac{1 + \omega}{1 - \omega}, \quad (26)$$

$$S = \frac{\omega}{1 - \omega^2} (p_r + \hat{\rho}) + \frac{1 + \omega^2}{1 - \omega^2} q + \epsilon \frac{1 + \omega}{1 - \omega}, \quad (27)$$

and the flux variable

$$\tilde{p} = \frac{p_r - \hat{\rho}\omega^2}{1 - \omega^2} + \frac{2\omega q}{1 - \omega^2} + \epsilon \frac{1 + \omega}{1 - \omega}, \quad (28)$$

as in the standard ADM 3+1 formulation. Within the PQSA  $\tilde{\rho}$  and  $\tilde{p}$  are referred as effective density and effective pressure, respectively.

Equations (22)–(25) are formally the same as for an anisotropic fluid, with  $\hat{\rho} = \rho + \rho_e$ ,  $p_r = p - \rho_e$ ,  $p_t = p + \rho_e$  and the electric energy density  $\rho_e = E^2/8\pi$ , where  $E = s/r^2$  is the local electric field intensity. If we define the degree of local anisotropy induced by charge as  $\Delta = p_t - p_r = 2\rho_e$ , the electric charge determines such a degree at any point.

From (22) and (25) we easily obtain

$$\frac{d\mu}{dt} = -4\pi r^2 \left\{ \frac{dr}{dt} p_r + [q + \epsilon(1 + \omega)] (1 - 2\mu/r)^{1/2} e^{\nu/2} \right\}. \quad (29)$$

This equation, known as the momentum constraint in the ADM 3+1 formulation, expresses the power across any moving spherical shell.

It can be shown that

$$\begin{aligned} & \tilde{p}_{,r} + \frac{(\tilde{\rho} + \tilde{p})(4\pi r^3 \tilde{p} + \mu)}{r(r-2\mu)} + \frac{2}{r}(\tilde{p} - p_t) \\ &= \frac{e^{-\nu}}{4\pi r(r-2\mu)} \left( \mu_{,tt} + \frac{3\mu_{,t}^2}{r-2\mu} - \frac{\mu_{,t}\nu_{,t}}{2} \right). \end{aligned} \quad (30)$$

This equation is the same as for an anisotropic fluid [75] and is a generalization of the hydrostatic support equation, that is, the Tolman–Oppenheimer–Volkoff (TOV) equation. Equation (30) is equivalent to the equation of motion for the fluid in conservative form in the standard ADM 3+1 formulation [26]. Equation (30) leads to the third equation at the surface (see next section); up to this point is completely general within spherical symmetry.

To close this sub-section we have to mention that we assume the following equation of state (EoS) [76] for nonadiabatic modeling and only as initial-boundary datum:

$$p_t - p_r = \frac{C(\tilde{p} + \tilde{\rho})(4\pi r^3 \tilde{p} + \mu)}{(r-2\mu)}, \quad (31)$$

where  $C$  is a constant.

### C. Junction conditions

We describe the exterior spacetime by the Reissner–Nordström–Vaidya metric

$$\begin{aligned} ds_+^2 &= \left( 1 - \frac{2\mathcal{M}(u)}{r} + \frac{\ell^2}{r^2} \right) du^2 + 2du dr \\ &\quad - r^2 (d\theta^2 + \sin^2 \theta d\phi^2), \end{aligned} \quad (32)$$

where  $\mathcal{M}(u)$  is the total mass and  $\ell$  the total charge, and  $u$  is the retarded time. The exterior and interior solutions are separated by the surface  $r = a(t)$ . In order to match both regions on this surface we use the Darmois junction conditions. Demanding the continuity of the first fundamental form, we obtain

$$e^{-\lambda_a} = 1 - \frac{2\mathcal{M}}{a} + \frac{\ell^2}{a^2}, \quad (33)$$

$$s_a = \ell, \quad (34)$$

$$m_a(u) = \mathcal{M} \quad (35)$$

and

$$\nu_a = -\lambda_a. \quad (36)$$

The subscript  $a$  indicates that the quantity is evaluated at the surface. In this work, we will use the continuity of the independent components of the energy-momentum flow instead of the second fundamental form, which have been shown to be equivalent [34] and it is simpler to apply to the present case. This last condition guarantees the absence of singular behaviors on the surface. It is easy to check that

$$p_a = q_a, \quad (37)$$

which expresses the continuity of the radial pressure across the boundary of the distribution  $r = a(t)$ .

#### D. Surface equations

Following the protocol sketched in [15] we write the surface equations evaluating (12), (29) and (30) at the surface of the distribution. The first and second surface equations read

$$\frac{da}{dt} = \omega_a \left( 1 - \frac{2\mu_a}{a} \right), \quad (38)$$

$$\frac{d\mu_a}{dt} = -L + \frac{\ell^2}{2a^2} \frac{da}{dt}, \quad (39)$$

with

$$L \equiv [Q + E(1 + \omega_a)] \left( 1 - \frac{2\mu_a}{a} \right), \quad (40)$$

where  $E = 4\pi a^2 \epsilon_a$  and  $Q = 4\pi a^2 q_a$ .

We need a third surface equation to specify the dynamics completely for any set of initial conditions and a given luminosity profile  $L(t)$ . For this purpose we can use the field Eq. (18) or the conservation Eq. (30) written in terms of the effective variables, which is clearly model dependent.

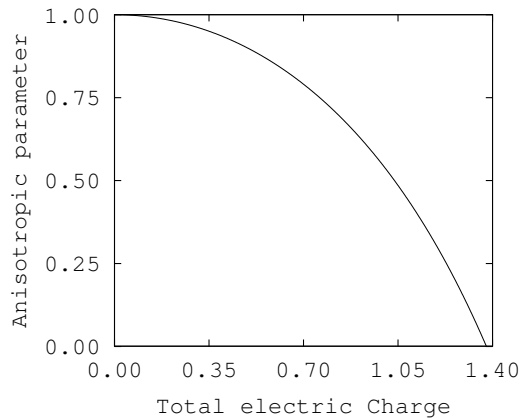


FIG. 1: Anisotropic parameter  $h$  as a function of the total electric charge  $\ell$ , calculated using (31) evaluated at the surface for the Schwarzschild-like model. The initial conditions are  $a(0) = 5.0$ ,  $m_a(0) = 1.0$ ,  $\omega_a(0) = -10^{-3}$ .

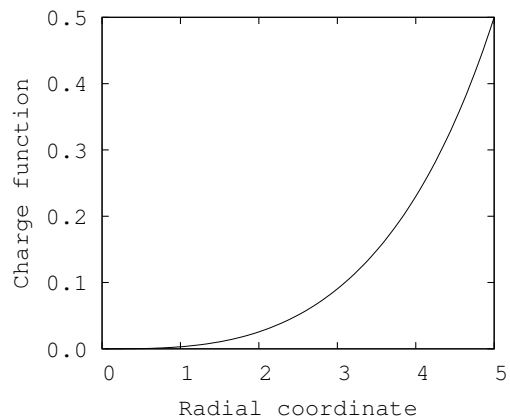


FIG. 2: Initial profile of the charge function  $s$ , calculated using (31) for the Schwarzschild-like model. The initial conditions are  $a(0) = 5.0$ ,  $m_a(0) = 1.0$ ,  $\omega_a(0) = -10^{-3}$ , with  $\ell = 0.5$ , which corresponds to  $h = 0.8966$ .

### III. NUMERICAL METHODS

Once the surface equations are integrated using a standard method, as Runge-Kutta of 4th order (RK4), we have to integrate the conservation equation (11) to obtain all the physical variables inside the source. Thus the conservation equation

$$s_{,t} = -\frac{dr}{dt} s_{,r}, \quad (41)$$

is a wave-like equation that can be integrated numerically using the Lax method (with the appropriate Courant-Friedrichs-Levy (CFL) condition). The evolution of the conservation equation is restricted by the sur-

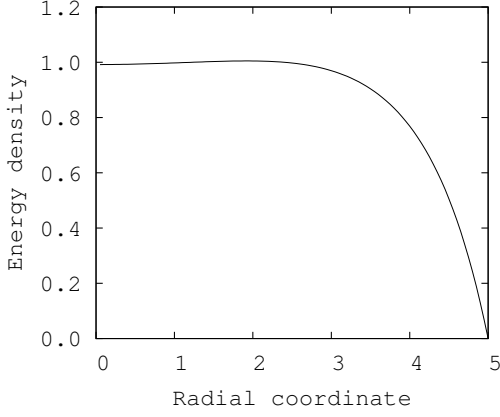


FIG. 3: Initial profile of the energy density  $\rho$  (a variation relative to the outermost value, multiplied by  $10^6$ ) for the Schwarzschild-like model I. The initial conditions are  $a(0) = 5.0$ ,  $m_a(0) = 1.0$ ,  $\omega_a(0) = -10^{-3}$ , with  $\ell = 0.5$ , which corresponds to  $h = 0.8966$ .

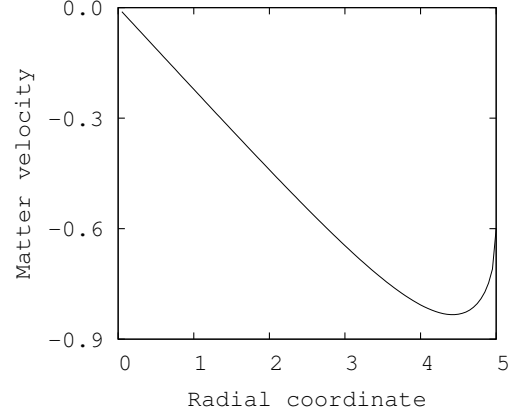


FIG. 5: Initial profile of the matter velocity  $dr/dt$  (multiplied by  $10^3$ ) for the Schwarzschild-like model I. The initial conditions are  $a(0) = 5.0$ ,  $m_a(0) = 1.0$ ,  $\omega_a(0) = -10^{-3}$ , with  $\ell = 0.5$ , which corresponds to  $h = 0.8966$ .

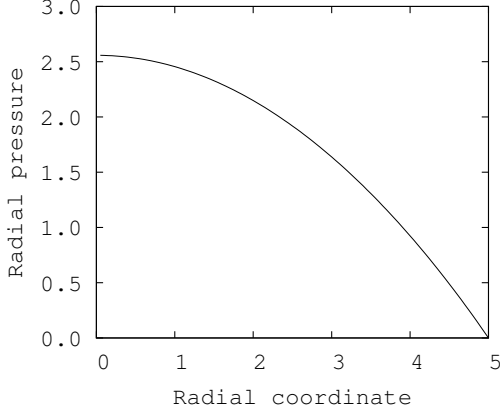


FIG. 4: Initial profile of the radial pressure  $p$  (multiplied by  $10^4$ ) for the Schwarzschild-like model I. The initial conditions are  $a(0) = 5.0$ ,  $m_a(0) = 1.0$ ,  $\omega_a(0) = -10^{-3}$ , with  $\ell = 0.5$ , which corresponds to  $h = 0.8966$ .

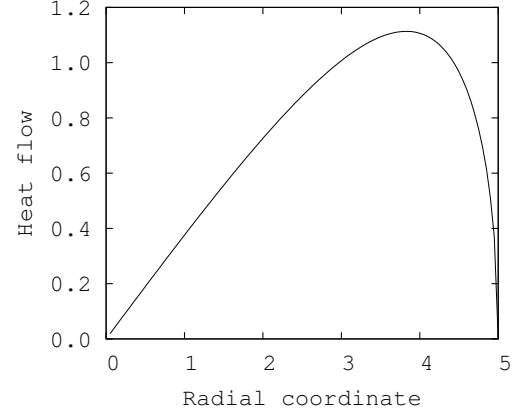


FIG. 6: Initial profile of the heat flow  $q$  (multiplied by  $10^6$ ) for the Schwarzschild-like model I. The initial conditions are  $a(0) = 5.0$ ,  $m_a(0) = 1.0$ ,  $\omega_a(0) = -10^{-3}$ , with  $\ell = 0.5$ , which corresponds to  $h = 0.8966$ .

face evolution and is implemented as follows

$$s_j^{n+1} = \frac{1}{2} (s_{j+1}^n + s_{j-1}^n) - \frac{\delta t}{2\delta r} \left( \frac{dr}{dt} \right)_j^n (s_{j+1}^n - s_{j-1}^n). \quad (42)$$

The superscript  $n$  indicates the hypersurface  $t = n\delta t$  and the subscript  $j$  the spatial position for a comoving observer at  $r = j\delta r$ . In order to integrate the conservation equation we need to specify a boundary-initial condition.

The PQSA is a seminumerical method where the radial dependence is determined from a static interior solution and kept the same during the evolution. The problem is typically reduced to a system of ordinary differential equations (ODEs) at the surface of the distribution of matter. This system is integrated in time using the RK4 method. Therefore we can calculate exactly any physi-

cal variable at the interior. In our specific case, for the Einstein-Maxwell system, the approach requires additionally the integration of the conservation of the electric charge (Eq. (41)) using the Lax method (Eq. (42)). The conservation equation is an evolution equation constrained by the system of ODEs at the surface. Thus, the numerical convergence of the whole algorithm must be of 2nd order accuracy.

The implemented algorithm at the surface (basically that of RK4) for the specific models was verified with satisfaction from a physical point of view and within a reasonable numerical error (see subsection IV.A). If the numerical solution for the electric charge function is stable and globally convergent to 2nd order, as shown in subsection IV.B, the problem surely is well-posed [77].

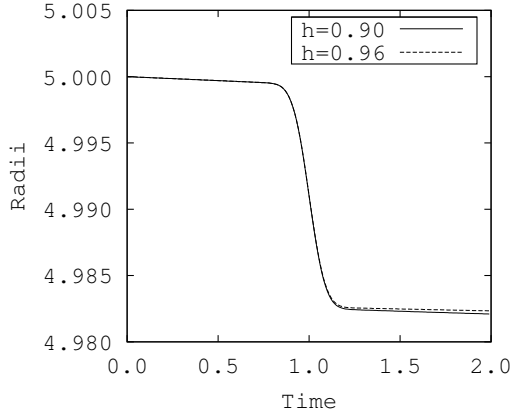


FIG. 7: Evolution of radius  $a$  for the Schwarzschild-like model I. The initial conditions are  $a(0) = 5.0$ ,  $m_a(0) = 1.0$ ,  $\omega_a(0) = -10^{-3}$ , with  $h = 0.90$  and  $h = 0.96$ , corresponding to  $\ell = 0.491$  and  $\ell = 0.314$ , respectively.

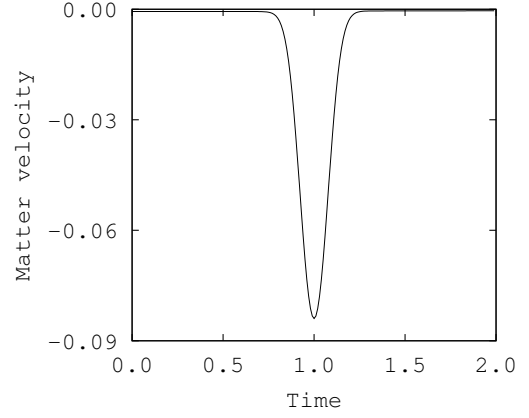


FIG. 9: Evolution of the matter velocity  $dr/dt$  at the surface for the Schwarzschild-like model I. The initial conditions are  $a(0) = 5.0$ ,  $m_a(0) = 1.0$ ,  $\omega_a(0) = -10^{-3}$ , with  $\ell = 0.5$ , which corresponds to  $h = 0.8966$

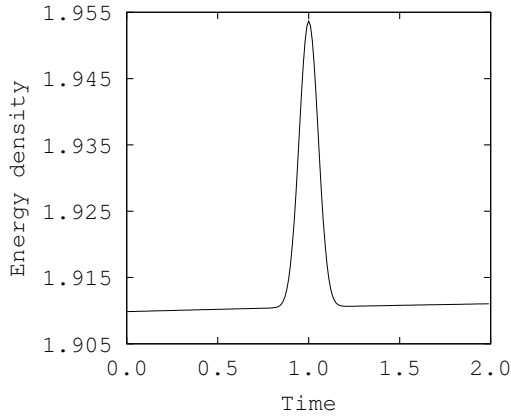


FIG. 8: Evolution of the energy density  $\rho$  (multiplied by  $10^3$ ) at the surface for the Schwarzschild-like model I. The initial conditions are  $a(0) = 5.0$ ,  $m_a(0) = 1.0$ ,  $\omega_a(0) = -10^{-3}$ , with  $\ell = 0.5$ , which corresponds to  $h = 0.8966$

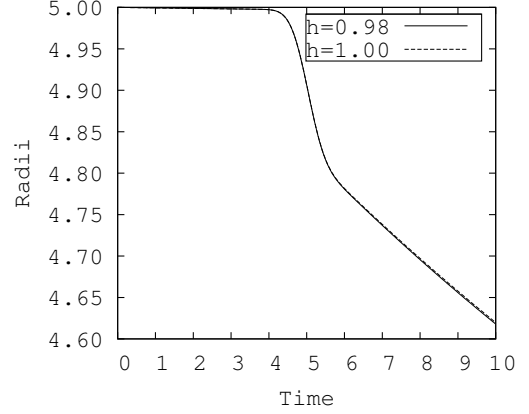


FIG. 10: Evolution of radius  $a$  for the Schwarzschild-like model II. The initial conditions are  $a(0) = 5.0$ ,  $m_a(0) = 1.0$ ,  $\omega_a(0) = -10^{-3}$ , with  $h = 0.98$  and  $h = 1$  corresponding to  $\ell = 0.222$  and  $\ell = 0$ , respectively.

#### IV. TESTING AND MODELING

To illustrate the method let us consider a Schwarzschild-like model. Following the protocol for the PQSA [15], [73] the interior solution has the effective density

$$\tilde{\rho} = f(t), \quad (43)$$

where  $f$  is an arbitrary function of time. The expression for  $\tilde{p}$  is

$$\frac{\tilde{p} + \frac{1}{3}\tilde{\rho}}{\tilde{p} + \tilde{\rho}} = \left(1 - \frac{8\pi}{3}\tilde{\rho}r^2\right)^{h/2} k(t), \quad (44)$$

where  $k$  is a function of  $t$  to be defined from the boundary condition (37), which now reads, in terms of the effective

variables, as

$$\tilde{p}_a = \tilde{\rho}_a \omega_a^2 + (q_a + \epsilon_a)(1 + \omega_a)^2 - (1 + \omega_a^2) \frac{\ell^2}{8\pi a^4}. \quad (45)$$

Thus, (44) and (45) give

$$\tilde{\rho} = \frac{3\mu_a}{4\pi a^3}, \quad (46)$$

$$\tilde{p} = \frac{\tilde{\rho}}{3} \left\{ \frac{\chi_S(1 - 2\mu_a/a)^{h/2} - 3\psi_S\xi}{\psi_S\xi - \chi_S(1 - 2\mu_a/a)^{h/2}} \right\}, \quad (47)$$

with

$$\xi = \left[1 - \frac{2\mu_a}{a}(r/a)^2\right]^{h/2}$$

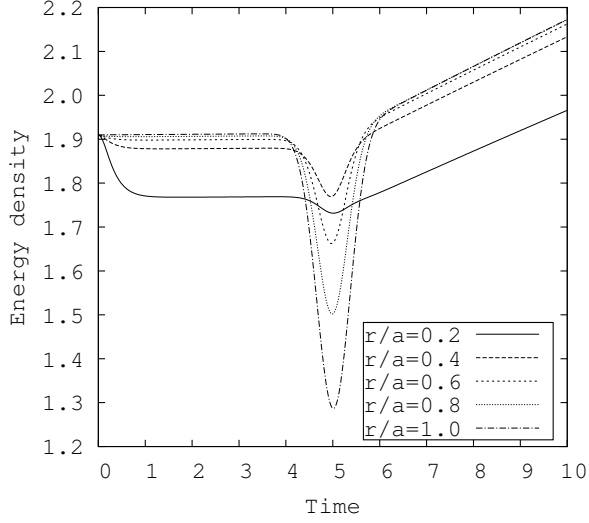


FIG. 11: Evolution of the energy density  $\rho$  (multiplied by  $10^3$ ) for the Schwarzschild-like model II. The initial conditions are  $a(0) = 5.0$ ,  $m_a(0) = 1.0$ ,  $\omega_a(0) = -10^{-3}$ , with  $\ell = 0.2$ , which corresponds to  $h = 0.9839$ .

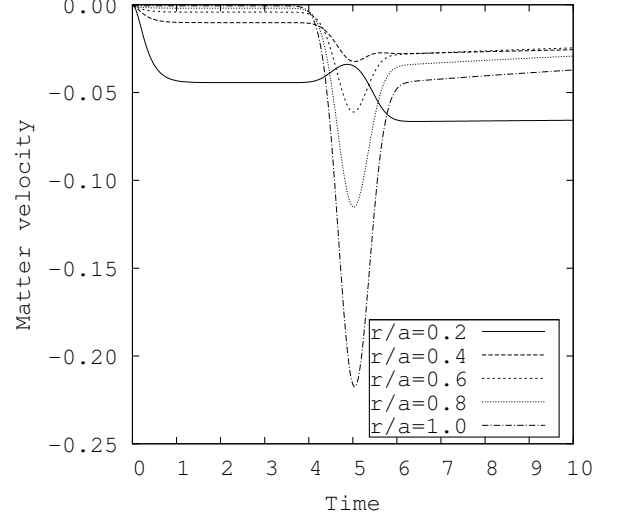


FIG. 13: Evolution of the matter velocity  $dr/dt$  for the Schwarzschild-like model II. The initial conditions are  $a(0) = 5.0$ ,  $m_a(0) = 1.0$ ,  $\omega_a(0) = -10^{-3}$ , with  $\ell = 0.2$ , which corresponds to  $h = 0.9839$ .

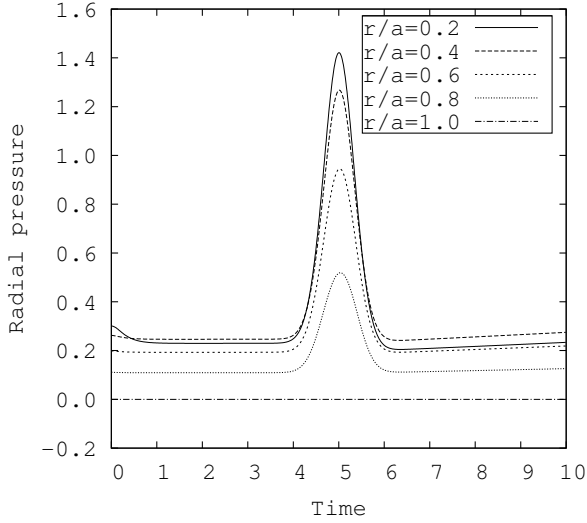


FIG. 12: Evolution of the radial pressure  $p$  (multiplied by  $10^3$ ) for the Schwarzschild-like model II. The initial conditions are  $a(0) = 5.0$ ,  $m_a(0) = 1.0$ ,  $\omega_a(0) = -10^{-3}$ , with  $\ell = 0.2$ , which corresponds to  $h = 0.9839$ .

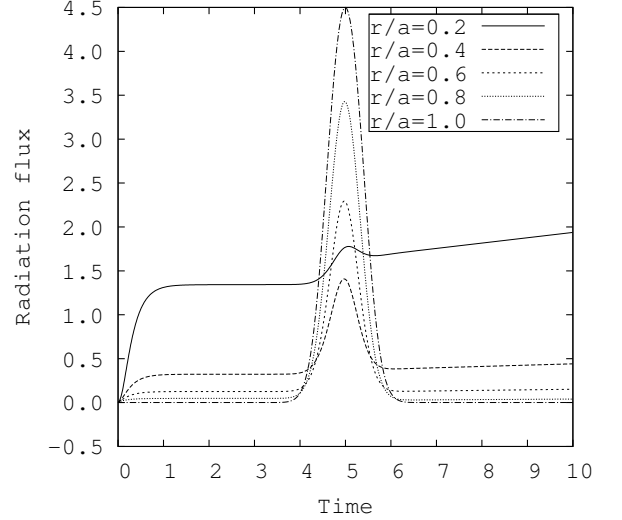


FIG. 14: Evolution of the radiation flux  $\epsilon$  (multiplied by  $10^4$ ) for the Schwarzschild-like model II. The initial conditions are  $a(0) = 5.0$ ,  $m_a(0) = 1.0$ ,  $\omega_a(0) = -10^{-3}$ , with  $\ell = 0.2$ , which corresponds to  $h = 0.9839$ .

where  $h = 1 - 2C$

$$\chi_S = 6(\omega_a^2 + 1)\frac{\mu_a}{a} + 2(Q + E)(1 + \omega_a)^2 - (1 + \omega_a^2)\frac{\ell^2}{a^2}, \quad (48)$$

and

$$\psi_S = 2(3\omega_a^2 + 1)\frac{\mu_a}{a} + 2(Q + E)(1 + \omega_a)^2 - (1 + \omega_a^2)\frac{\ell^2}{a^2}. \quad (49)$$

Using (22) and (23) it is easy to obtain expressions for  $\mu$  and  $\nu$ :

$$\mu = \mu_a(r/a)^3, \quad (50)$$

$$e^\nu = \left\{ \frac{a[\chi_S(1 - 2\mu_a/a)^{h/2} - \psi_S\ell]}{4\mu_a} \right\}^{2/h}, \quad (51)$$



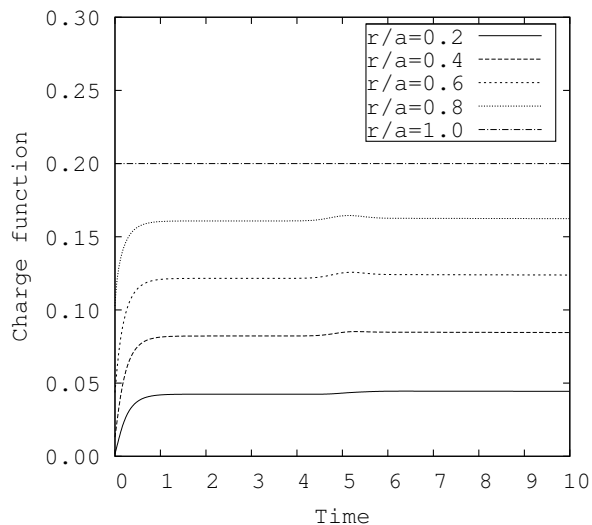


FIG. 15: Evolution of the charge function  $s$  for the Schwarzschild-like model II. The initial conditions are  $a(0) = 5.0$ ,  $m_a(0) = 1.0$ ,  $\omega_a(0) = -10^{-3}$ , with  $\ell = 0.2$ , which corresponds to  $h = 0.9839$ .

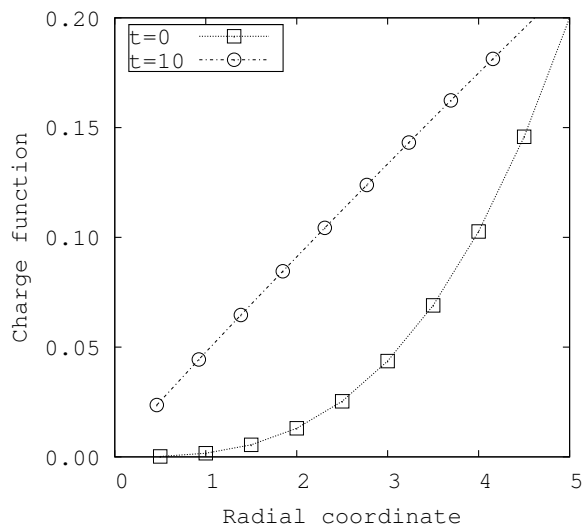


FIG. 16: Initial and final charge function  $s$  profile for the Schwarzschild-like model II. The initial conditions are  $a(0) = 5.0$ ,  $m_a(0) = 1.0$ ,  $\omega_a(0) = -10^{-3}$ , with  $\ell = 0.2$ , which corresponds to  $h = 0.9839$ .

which correspond to the Hamiltonian constraint and to the polar slicing condition in the ADM 3+1 formulation, respectively. It is necessary to specify one function of  $t$  and the initial data.

We choose  $L(t)$  to be a Gaussian

$$L = L_0 e^{-(t-t_0)^2/\Sigma^2}, \quad (52)$$

with  $L_0 = M_r/\sqrt{\Sigma\pi}$ , which corresponds to a pulse radiating away a fraction of the initial mass  $M_r$ . It is easy

to construct the initial profile for the charge function. From (31) evaluated at the surface we obtain  $h(\ell)$  (see Figure 1). Figure 2 displays the charge function  $s$  for the following set of initial conditions

$$a(0) = 5, \quad m_a(0) = 1, \quad \omega_a(0) = -10^{-3}, \quad (53)$$

with  $\ell = 0.5$ , which corresponds to  $h = 0.8966$ .

### A. Model I

In the diffusion limit ( $\epsilon = 0$ ) we choose  $t_0 = 1.0$  and  $\Sigma = 0.01$ ,  $M_r = 10^{-2}$ . We tested that the algorithm is correct at the surface (that is, locally) by verifying that the pressure is equal to the given gaussian pulse with an accuracy of about  $10^{-19}$ . This allow us at least to be confident about the implemented algorithm at the surface. However, as a double-check, from an strictly numerical point of view, we show in Table I a proper convergence test to 4th order of the RK algorithm at the surface. For this test we use the gravitational potential at the surface as the required norm,  $\mathcal{N} = \mu_a/a$ . Thus, it can be shown that the rate of convergence is

$$n = \log_2 \frac{\mathcal{N}_c - \mathcal{N}_m}{\mathcal{N}_m - \mathcal{N}_f}, \quad (54)$$

where  $\mathcal{N}_c$ ,  $\mathcal{N}_m$  and  $\mathcal{N}_f$  are values of  $\mathcal{N}$  for a coarse, medium, and fine time step  $\Delta t$ , respectively (scaling as 4:2:1, [78],[79]). This corresponds to a local convergence test for the RK4, giving a convergence rate  $n \approx 4$ , as expected.

$t$	$\mathcal{N}_c - \mathcal{N}_m (10^{-10})$	$\mathcal{N}_m - \mathcal{N}_f (10^{-12})$	$n$
1.0	-0.022	-0.142	3.964
1.5	-0.573	-3.586	3.998
2.0	-1.148	-7.180	3.999

TABLE I: Proper convergence of the surface gravitational potential; the expected value for  $n$  is 4.

For the initial setting corresponding to Figure 2 the interior does not evolve because the velocity becomes a complex value. However, we can display for analysis the initial set of physical variables in Figures 3–6. Under these conditions the surface evolves without anomalies as shown in Figures 7–9. We have looked for an electrically charged initial configuration for which all regions evolve; we found one with a total electric charge  $\approx 10^{-6}$ .

### B. Model II

Let us consider now a Schwarzschild-like model in the streaming-out limit ( $q = 0$ ). We choose  $t_0 = 5.0$  and  $\Sigma = 0.25$ ,  $M_r = 10^{-1}$ . We tested again that the algorithm is

correct at the surface by verifying that the pressure is equal to zero with an accuracy of about  $10^{-19}$ . For this model we show the global rate of proper convergence in Table II. For that purpose we construct the following norm with the electric charge function  $s$

$$\mathcal{N} = \int_0^a s^2 dr. \quad (55)$$

For instance, we choose grids of 10, 20 and 40 nodes,

$t (10^{-7})$	$\mathcal{N}_c (10^{-3})$	$\mathcal{N}_m (10^{-3})$	$\mathcal{N}_f (10^{-3})$	$n$
0	3.5423	3.5322	3.5297	2.0152
1	5.1726	5.1564	5.1524	2.0398

TABLE II: Proper convergence of the norm (55); the expected value for  $n$  is 2.

and a RK4 time step of  $10^{-8}$  in a proportion of 4:2:1, respectively. To reach the same monitoring time the CFL time step have to be  $\delta t = K \delta r$ , where  $K$  is a constant of order of one, in proportion 4:2:1 as well. Consequently, the number of RK4 time steps required to apply the formula (54) is in proportion 1:4:16. The global convergence test (RK4 + Lax) gives a rate of  $n \approx 2$ , as expected.

The initial setting shown in Figure 2 is valid for this model too, but with  $\ell = 0.2$  (corresponding to  $h = 0.8966$ ). A larger total electric charge does not allow an interior evolution because unphysical values develop. Figures 10–16 show these results. The collapse is unavoidable after emitting an energy equivalent to 10 % of the initial mass, which decreases the energy density (the contrary occurs in the diffusion limit [80]). The electric charge is redistributed in the whole body. Note that the electric charge on each comoving shell starts moving until it reaches a stationary state while the whole distribution collapses. Observe how the gradient of charge decreases and becomes linear with the advance of time.

## V. CONCLUDING REMARKS

We consider the evolution of a self-gravitating spherical distribution of charged matter containing a dissipative fluid. The use of the PQSA with noncomoving coordinates allows us to study electrically charged fluid spheres in the diffusion and the streaming out limits as they just depart from equilibrium. From this point of view, the PQSA can also be seen as a nonlinear perturbative method to test the stability of solutions in equilibrium. We have shown that our seminumerical implementation is globally second-order convergent.

Our results indicate that the dissipative transport mechanisms and the equation of state chosen to treat electric charge as anisotropy are crucial for the outcome of gravitational collapse. We want to stress: i) the straightforward manner in which we connected anisotropy with electric charge using an EoS; ii) how the EoS is used in practice as an initial-boundary condition;

iii) that departing from the same static solutions we find very different evolutions. Increasing the amount of total charge  $\ell$  results in lower values of the anisotropy parameter  $h$ , approaching zero. The zero limit is not reached because the system breaks down for some limit value of the total electric charge. When the transport mechanism is diffusive, it was not possible to establish why the system can be set initially but not evolved, except at the surface. From the results, the field equations seem to be imposing restrictions within the context of diffusion and electric charge (or anisotropy) and permit only bubbles of charged matter. Otherwise the electric charge (or anisotropy) has to be very small. In the streaming out limit the situation is quite different, as is expected. The interior is evolved for a total charge that is 200,000 times that of the maximum charge permitted in the diffusion limit. Coupling of matter with radiation is not strong enough to prevent the collapse and the system efficiently radiates a large quantity of mass. The system clearly departs equilibrium and collapses. Electric charge contributes to the collapse in the same way that anisotropy with tangential pressure greater than radial pressure favors the collapse [73], irrespective of the transport mechanism. In any case electric charge has to be huge to change the fate of the gravitational collapse. The electric charge is redistributed in a such way that its gradient decreases toward the surface and becomes unexpectedly linear and stationary, with the advance of time. There is a critical total electric charge (or anisotropy parameter) for which the system evolves constrained by the Einstein–Maxwell system of field equations.

Beyond the models we want to stress some features about our framework. First, the luminosity profiles are given as Gaussian but they can be provided from observational data. To keep physical variables on appropriate values in the diffusion approximation, the pulse has to be narrow in comparison, while the streaming out limit allows for a wider pulse. Second, the EoS used in this work is not essential. Other EoS as initial-boundary data should fit well, understanding that it represents anisotropic matter. Third, from the observational point of view, temperature profiles are desirable as input data, but they are not available in the PQSA method when electric charge is taken in account.

We considered the dissipation by viscosity and heat flow separately [73], [80], in order to isolate similar effects with different mechanisms. In this work we considered heat flow/streaming out and anisotropy induced by electric charge, pointing to the most realistic numerical modeling in this area [35]. The results constitute a definite first cut to more general situations using the PQSA, including dissipation, anisotropy, electric charge, heat flow, viscosity, radiation flux, superficial tension, temperature profiles and study their influence on the gravitational collapse. Numerical issues apart, the inclusion of superficial tension [81] together with a highly compressed Fermi gas [15], and more realistic thermal processes [68], is of current interest in astrophysics [35]. Cooling times

of smooth or crusty surfaces may be the way to differentiate strange stars from neutron stars [47]. The PQSA can be used to model these situations. This investigation is an essential part of a long-term project which tries to incorporate the Müller–Israel–Stewart theory for dissipation and deviations from spherical symmetry, specially when considering electrically charged distributions. Besides being interesting in their own right, we believe that spherically symmetric fluid models are useful as a test bed for more general solvers in numerical relativity

[27, 28]. A general three-dimensional code must also be able to reproduce situations closer to equilibrium.

### Acknowledgments

C. P. acknowledges the computing resources provided by the Victorian Partnership for Advanced Computation (VPAC).

- 
- [1] C. Misner and D. Sharp, Phys. Rev. **136**, B571(1964).
  - [2] C. Ghezzi, Phys. Rev. D **72**, 104017 (2005).
  - [3] C. Ghezzi and P. Letelier, Phys. Rev. D **75**, 024020 (2007).
  - [4] M. M. May and R. H. White, Phys. Rev. **141**, 4 (1966).
  - [5] M. M. May and R. H. White, Methods in Computational Physics, **7**, 219 (1967).
  - [6] L. Lehner, Class. Quantum Grav. **18**, 25 (2001).
  - [7] M. W. Choptuik, Phys. Rev. Lett. **70**, 9 (1993).
  - [8] F. Pretorius, Phys. Rev. Lett. **95**, 121101 (2005).
  - [9] M. Campanelli, C. O. Lousto, P. Marronetti, and Y. Zlochower, Phys. Rev. Lett. **96**, 111101 (2006).
  - [10] J. G. Baker, J. Centrella, D.-I. Choi, M. Koppitz, and J. van Meter, Phys. Rev. Lett. **96**, 111102 (2006).
  - [11] L. Baiotti, B. Giacomazzo, and L. Rezzolla, Phys. Rev. D **78**, 084033 (2008).
  - [12] J. A. Font, “Numerical Hydrodynamics and Magnetohydrodynamics in General Relativity”, Living Rev. Relativ. **6**, (2003), URL (cited on 06 March 2010): <http://www.livingreviews.org/lrr-2008-7>
  - [13] J. Winicour, “Characteristic Evolution and Matching”, Living Rev. Relativity **12**, (2009), URL (cited on 01 May 2010): <http://www.livingreviews.org/lrr-2009-3>
  - [14] W. Barreto, B. Rodríguez, and H. Martínez, Ap. Sp. Sc., **282**, 581 (2002).
  - [15] L. Herrera, W. Barreto, A. Di Prisco, and N. Santos, Phys. Rev. D, **65** 104004 (2002).
  - [16] L. Herrera, J. Jiménez, and G. Ruggeri, Phys. Rev. D, **22**, 2305 (1980).
  - [17] L. Herrera and L. Núñez, Fund. Cosmic Phys., **14**, 235 (1990).
  - [18] W. Barreto and L. A. Núñez, Ap. Sp. Sc. **178**, 261 (1991).
  - [19] W. Barreto, L. Herrera, and L. Núñez, Ap. J. **375**, 663 (1991).
  - [20] W. Barreto, L. Herrera, and N. Santos, Ap. Sp. Sc. **187**, 271 (1992).
  - [21] R. Aquilano, W. Barreto, and L. A. Núñez, Gen. Rel. Grav. **26**, 537 (1994).
  - [22] L. Herrera, A. Melfo, L. A. Núñez, and A. Patiño, Ap. J. **421**, 677 (1994).
  - [23] V. Medina, L. Núñez, H. Rago, and A. Patiño, Can. J. Phys. **66**, 981 (1988).
  - [24] W. Barreto and A. Da Silva, Gen. Rel. Grav. **28**, 735 (1996).
  - [25] A. Patiño and H. Rago, Ap. Sp. Sc. **241**, 237 (1996).
  - [26] W. Barreto Phys. Rev. D **79**, 10, 107502 (2009).
  - [27] W. Barreto, L. Castillo, and E. Barrios Phys. Rev. D **80**, 084007 (2009).
  - [28] W. Barreto, L. Castillo, and E. Barrios, Gen. Rel. Grav. **42**, 1845 (2010).
  - [29] J. Bekenstein, Phys. Rev. D **4**, 2185 (1971).
  - [30] V. Shvartsman, Sov. Phys. JETP **33**, 475 (1971).
  - [31] E. Olson and M. Bailyn, Phys. Rev. D **13**, 2204 (1976).
  - [32] J. Bally and E. Harrison, Ap. J. **220**, 743 (1978).
  - [33] H. J. Mosquera Cuesta, A. Penna-Firme, and A. Pérez-Lorenzana, Phys. Rev. D **67**, 087702 (2003).
  - [34] L. Herrera and A. Di Prisco, Phys. Rev. D, **55**, 2044 (1997).
  - [35] A. Di Prisco, L. Herrera, G. Le Denmat, M. A. H. MacCallum, and N. O. Santos, Phys. Rev. D **76**, 064017 (2007).
  - [36] B. V. Ivanov, Phys. Rev. D **65**, 104001 (2002).
  - [37] V. Varela, Gen. Rel. Grav. **39**, 267 (2007).
  - [38] S. Ray, A. L. Espindola, M. Malheiro, J. P. S. Lemos, and V. T. Zanchin Phys. Rev. D **68**, 084004 (2003).
  - [39] J. P. S. Lemos and E. J. Winberg, Phys. Rev. D **69**, 104004 (2004); J. P. S. Lemos and V. T. Zanchin, *Quasi-black holes with pressure: relativistic charged spheres as the frozen stars*, arXiv:1004.3574.
  - [40] W. B. Bonnor, Gen. Rel. Grav. **42**, 1825 (2010).
  - [41] W. Barreto, B. Rodríguez, L. Rosales, and O. Serrano, Gen. Rel. Grav., **39**, 23 (2007); Errata **39** 537 (2007).
  - [42] B. V. Ivanov, Int. J. Theor. Phys. **49**, 1236 (2010); B. V. Ivanov, *The fundamental spherically symmetric fluid models*, arXiv: 0912.2447.
  - [43] S. Thirukkanesh and S. D. Maharaj, Class. Quantum Grav. **25** 235001 (2008).
  - [44] M. Esculpi and E. Alomá, Europ. Phys. J. C, *Conformal anisotropic relativistic charged fluid spheres with a linear equation of state*, published on line, April (2010)
  - [45] V. Usov, Phys. Rev. D **70**, 067301 (2004).
  - [46] M. Mak and T. Harko, Int. J. Mod. Phys. D **13**, 149 (2004).
  - [47] P. Jaikumar, S. Reddy, and A. W. Steiner, Phys. Rev. Lett. **96**, 041101 (2006).
  - [48] L. Herrera and N. O. Santos, Mon. Not. R. Astron. Soc., **343**, 1207 (2003).
  - [49] C. Hansen and S. Kawaler, *Stellar Interiors: Physical Principles, Structure and Evolution*, (Springer Verlag, Berlin, 1994).
  - [50] R. Kippenhahn and A. Weigert, *Stellar Structure and Evolution*, (Springer Verlag, Berlin, 1990); M. Schwarzschild, *Structure and Evolution of the Stars*, (Dover, New York, 1958).
  - [51] L. Herrera and N. O. Santos, Phys. Rev. D **70**, 084004 (2004).
  - [52] G. Lemaitre, Ann. Soc. Sci. Bruxelles A **53**, 51 (1933).
  - [53] L. Herrera and N. Santos, Phys. Rep. **286**, 53 (1997).

- [54] M. Esculpi, M. Malaver, and E. Alomá, *Gen. Rel. Grav.* **39**, 633 (2007).
- [55] L. Herrera, A. Di Prisco, J. Martín, J. Ospino, N.O. Santos, and O. Troconis, *Phys. Rev. D* **69**, 084026 (2004).
- [56] R. Tabensky and A. Taub, *Comm. Math. Phys.* **29** 61 (1973).
- [57] B. Tupper, *J. Math. Phys.*, **22**, 2666 (1981).
- [58] B. Tupper, *Gen. Rel. Grav.*, **15** 849 (1983).
- [59] A. Raychaudhuri and S. Saha, *J. Math. Phys.*, **22** 2237 (1981); A. Raychaudhuri and S. Saha, *J. Math. Phys.*, **23** 2554 (1982).
- [60] J. Carot and J. Ibáñez, *J. Math. Phys.* **26** 2282 (1985).
- [61] W. Barreto and S. Rojas, *Ap. Sp. Sc.*, **193** 201 (1992); W. Barreto, *Ap. Sp. Sc.*, **201** 191 (1993); A. A. Coley and B. O. J. Tupper, *Class. & Quantum Grav.*, **11** 2553 (1994).
- [62] B. Mashhoon and M. Partovi, *Phys. Rev. D* **20**, 2455 (1979).
- [63] D. Kazanas and D. N. Schramm, *Neutrino competition with gravitational radiation during collapse*, in *Sources of gravitational Radiation*, p. 345 (Ed. L. L. Smarr, Cambridge: Cambridge University Press, 1979).
- [64] J. Lattimer, *Nucl. Phys. A* **478**, 199 (1988).
- [65] J. Martínez, *Phys. Rev. D* **53**, 6921 (1996).
- [66] L. Herrera, A. Di Prisco, J. L. Hernández-Pastora, J. Martín, and J. Martínez, *Class. Quantum Grav.* **14**, 2239 (1997).
- [67] L. Herrera and J. Martínez, *J. Math. Phys.* **39**, 3260 (1998).
- [68] L. Herrera, A. Di Prisco, and W. Barreto, *Phys. Rev. D* **73**, 024008 (2006).
- [69] I. Müller, *Z. Phys.* **198**, 329 (1967).
- [70] W. Israel, *Ann. Phys.* **100**, 310 (1976).
- [71] W. Israel and J. M. Stewart, *Phys. Lett. A* **58**, 213 (1976).
- [72] W. Israel and J. M. Stewart, *Ann. Phys.* **118**, 341 (1979).
- [73] C. Peralta, L. Rosales, B. Rodríguez-Mueller, and W. Barreto, *Phys. Rev. D* **81**, 104021 (2010).
- [74] H. Bondi, *Proc. Royal Soc. London*, **A281**, 39 (1964).
- [75] M. Cosenza, L. Herrera, M. Esculpi, and L. Witten, *Phys. Rev. D* **25**, 2527 (1982).
- [76] W. Barreto, *Ap. Sp. Sc.* **201**, 191 (1993).
- [77] This is an important theoretical and numerical issue; we thank the referee for bringing it up to our attention.
- [78] N. T. Bishop, R. Gómez, S. Husa, L. Lehner, and J. Winicour, *Phys. Rev. D* **68**, 084015 (2003).
- [79] W. Barreto, A. Da Silva, R. Gómez, L. Lehner, L. Rosales, and J. Winicour, *Phys. Rev. D* **71**, 064028 (2005).
- [80] B. Rodríguez-Mueller, C. Peralta, W. Barreto, and L. Rosales *Heat flow in the postquasistatic approximation*, to appear in *Phys. Rev. D* (2010); arXiv:1005.1637
- [81] L. Herrera, J. Jiménez, M. Esculpi, and J. Ibáñez, *Ap. J.* **345** 918 (1989).